

Design of Electric Differential System for an Electric Vehicle with Dual Wheel Motors

Yee-Pien Yang, *Member, IEEE*, Xian-Yee Xing

Abstract—This paper proposes an electric differential system (EDS) for an electric vehicle (EV) driven directly by dual motors in the rear wheels. This system consists of twofold control loops: the outer loop modulates the yaw motion of the vehicle, and the inner loop improves the robustness against system uncertainties and road conditions. In experiments, the inner control loop is constructed by using MATLAB®/Simulink® software performed on a laptop, while the outer control loop is realized with an EPF10KE Field Programmable Gate Array (FPGA) in the fixed-point arithmetic format. The effectiveness of the proposed EDS is successfully demonstrated by a straight-line test with a commercial vehicle, which is reconstructed to be driven directly by two rear wheel motors.

I. INTRODUCTION

IN recent years, environmental protection concerns and energy conservation issues are so critical that many researchers and major manufacturers have put forth great effort to develop high-performance and low-pollution electric vehicles (EVs) to replace the conventional vehicles with internal combustion engines. Pure and hybrid EVs use energy storage elements, such as batteries, to generate electric energy and then transform it into mechanical energy by electrical motors to yield a required driving power. Therefore, they have less tailpipe emission and less consumption of petroleum [1, 2].

From the perspective of control engineering, the EVs have many advantages:

- 1) Electric motors can generate fast torque response.
- 2) Electric motor torque can be measured precisely.
- 3) More than one motor can be mounted on each vehicle, and can be controlled independently.

Consequently, some advanced vehicle control methods have been realized to improve the handling and stability of vehicles, especially in severe driving situations [3, 4]. Hori *et al.* [5] developed an electric differential system (EDS) using the concept of model following control (MFC) to minimize tire slip when the vehicle was running on a low-friction road. This approach was imprecise even though the tire and road

adhesion was increasingly enhanced. On the basis of an optimal slip ratio controller (SRC), Sado *et al.* [6] designed an EDS to improve vehicle stability by maintaining the slip ratio within an ideally specified region. This scheme was exquisite, although it required the information of vehicle speed to estimate the slip ratio.

Although the vehicle speed could be obtained by measuring the acceleration of the chassis, or approximately derived from the rotational speed of wheels, these approximations were erroneous in certain situations, such as braking or cornering [7]. Fujii *et al.* [8] offered a slip ratio observer (SRO) to complete an EDS containing a SRC without detecting the vehicle speed. However, the SRO relied on a linear model, and did not function well in the non-linear region. Fujimoto *et al.* [9] presented a novel EDS containing double disturbance observers (DOB) accompanied with a dead-time generator to enhance driving safety. Meanwhile, many strategies have required expensive sensors to detect side slip angle for the EDS to construct their closed-loop structure [10, 11]. In other cases, some researchers may have improperly complicated the control structure by adding a side slip angle observer [12] or even by avoiding this information [13,14]. Therefore, their control algorithms of EDS become so complex that real-time implementation becomes difficult.

Even though research on the EDS of EVs has been ongoing for years, some critical issues are rarely discussed. For instance, if the dynamics of driving motors are inconsistent, perhaps owing to defects in fabrication, the handling of the vehicle can be greatly influenced, so that the driver has to make more effort to keep the vehicle running straight while driving on a rectilinear path. On the other hand, road conditions may cause such severe and unbalanced loads on wheels that factors influencing the stability and controllability of the vehicle become much more important in the advanced development of EVs.

This paper proposes a simplified EDS, without expensive sensors, for an EV driven by dual rear wheels. The proposed EDS has twofold control loops to improve driving safety and stability. The outer control loop supervises the yaw motion of vehicle through a laptop. The inner loop finely tunes the wheel speed against external disturbances and system uncertainties by the model reference adaptive control (MRAC) approach on the basis of Lyapunov stability theory. The MRAC algorithms are realized by utilizing an EPF10KE Field Programmable Gate Array (FPGA) and coded with the Verilog hardware description language (Verilog HDL) in fixed-point arithmetic format, to expedite the execution of program with minimal usage of hardware and software resources. Its major

This work was supported by the National Science Council of Taiwan, R.O.C., under contract NSC95-2218-E-002-020.

Y. P. Yang, corresponding author, is with the Department of Mechanical Engineering, National Taiwan University (Tel: +886-2-3366-2682; fax: +886-2-2363-1755; e-mail: ypyang@ntu.edu.tw).

X. Y. Xing, was with the Department of Mechanical Engineering, National Taiwan University. He is now in a military service. (Tel: +886-2-3366-2771; fax: +886-2-2363-1755; e-mail: r94522821@ntu.edu.tw).

advantage is to assist drivers to handle most road conditions, so that the driver may focus on a path-following task that is subject to undesirable uncertainties and disturbances. Finally, the effectiveness of the proposed EDS is demonstrated with an experimental vehicle “Nissan March”, which was reconstructed to be driven directly by two wheel motors, as shown in Fig. 1.



Fig. 1. The experimental vehicle (a) and its wheel motor (b).

II. ELECTRONIC DIFFERENTIAL SYSTEM (EDS)

The proposed EDS consists of an outer control loop and an inner control loop. The outer control loop oversees the yaw motion to prevent vehicle side slip, while the current commands to the rear driving wheels are determined for the inner control loop. The inner loop converts the torque command for each motor to a current resulting in a compromise between the two rear wheels to exert a correct yaw moment by adjusting their differential speeds. The bicycle and linear longitudinal models of a vehicle are used in the outer and inner control loop, respectively, to describe the lateral, longitudinal and yaw motion of the vehicle. It is necessary to make the following assumptions:

- 1) The vehicle speed is constant when cornering.
- 2) The steering angles of the two front wheels are equivalent.
- 3) The air adhesion and rolling resistance are ignored.
- 4) The front tires have the same side slip angle, so do the rear tires.
- 5) Complete adhesion or no slip on tires is assumed.

A. Outer Control Loop

The well-known bicycle model, as illustrated in Fig. 2, is used to describe the linear dynamics of vehicle chassis in the lateral, longitudinal, and yaw directions. The corresponding governing equations are expressed as [15]

$$\frac{d\beta}{dt} = a_{11}\beta + a_{12}\gamma + e_1\delta \quad (1)$$

$$\frac{d\gamma}{dt} = a_{21}\beta + a_{22}\gamma + e_2M + e_3\delta \quad (2)$$

where

$$a_{11} = \frac{-2(C_f + C_r)}{mV_x}, \quad a_{12} = -1 - \frac{2(l_f C_f - l_r C_r)}{mV_x^2},$$

$$a_{21} = \frac{-2(l_f C_f - l_r C_r)}{I_z}, \quad a_{22} = \frac{-2(l_f^2 C_f - l_r^2 C_r)}{I_z V_x},$$

$$e_1 = \frac{-2C_f}{mV_x}, \quad e_2 = \frac{1}{I_z}, \quad e_3 = \frac{2l_f C_f}{I_z}.$$

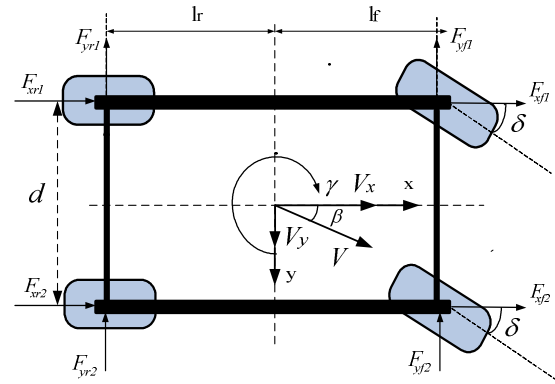


Fig. 2. Lateral vehicle model.

Here, β is the side slip angle of vehicle, which is defined as the angle between the directions of the vehicle velocity and its chassis. The yaw rate of the chassis is denoted by γ , the front steering angle is δ , and the coefficients a 's and e 's are functions of the cornering stiffness C_f and C_r of the front and rear tires, the moment of inertia I_z in the direction of yaw motion, the vehicle mass m , and the vehicle velocity V_x in the x -direction. Notice that the coordinate x - y is fixed on the vehicle.

In the ideal situation when the side slip angle of vehicle is zero, the desired yaw rate at the centre of gravity in the steady state relates to the steering angle with a simplified first-order transfer function:

$$\gamma_d = \frac{K_y}{1 + \tau \cdot s} \delta \quad (3)$$

where the steady gain K_y can be easily expressed as a function of a 's and e 's in (1) and (2), and the time constant τ can be regarded as a design parameter and is determined according to engineers' experience. Detailed derivation is referred to the research of Shino *et al.* [16].

The yaw rate control loop is devised as shown in Fig. 3, where a conventional PI controller is applied to reduce the steady state error between the desired yaw rate and the real yaw rate measured by a yaw rate sensor. The gain $K_{C/T}$ scales the throttle command into a suitable level; the PI gain is also tuned accordingly that the resultant current commands for the left and right driving wheels are realizable for software programming. This pair of current commands, CCL and CCR, enters into the inner loop to regulate the differential speeds of two driving wheels, thereby producing a correct yaw moment to satisfy the desired yaw rate.

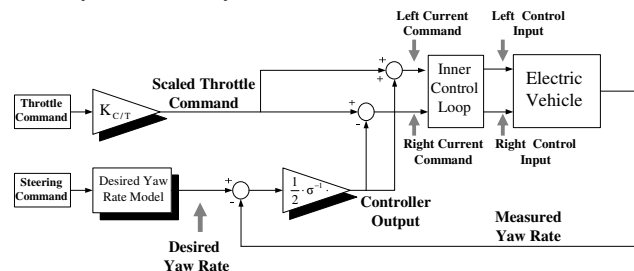


Fig. 3. Block diagram of yaw rate control loop.

B. Inner Control Loop

The inner control loop is responsible for finely tuning the differential speed of driving wheels, either to eliminate the side slip of vehicle when running along straight lane, or to produce a desired yaw rate when cornering, subject to system uncertainties and external disturbances. A major system uncertainty comes from the unequal dynamics of driving motors due to manufacturing defects or installation inaccuracy, while the external disturbance depends mainly on the road condition.

For each driving wheel, as depicted in Fig. 4, under the assumption of complete adhesion, the linear longitudinal vehicle dynamics without slip can be expressed as

$$(J_w + Mr_w^2) \frac{d\omega}{dt} + b \omega = T \tag{4}$$

where J_w is the mass moment of inertia of the wheel, including the driving motor, the tire and the shaft; M is a quarter of vehicle mass; r_w is the wheel radius; ω is the rotational speed of wheel; and b denotes the viscous damping coefficient. The torque T produced by wheel motor is simply expressed as $T = K_T I_c$, where K_T is the torque constant, and I_c is the current command.

When slip occurs on a low friction road, it can be viewed as a sudden decrease of the inertia Mr_w^2 [17] and thus the wheel speed changes immediately endangering the driver's safety. Similarly, the influence from disturbances or system uncertainties can be also regarded as inertia fluctuation to affect the wheel speed. In summary, the mass moment of inertia of the one wheel model lumps to

$$J = J_w + Mr_w^2 (1 + \Delta) \tag{5}$$

where Δ represents the variation of inertia, while $J_n = J_w + Mr_w^2$ becomes the nominal mass moment of inertia.

Accordingly, the transfer function of the plant $P(s)$, which approximates the real longitudinal vehicle dynamics, in the inner control loop as shown in Fig. 5, describes the relationship between the wheel speed and current command as follows

$$P(s) = \frac{\omega}{u_c}(s) = \frac{K_T}{Js + b} \tag{6}$$

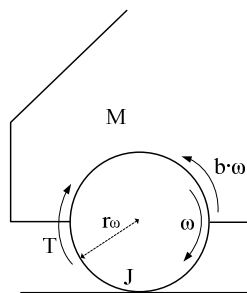


Fig. 4. Longitudinal vehicle model.

Similarly, the transfer function $P_m(s)$ between the reference speed and current command is denoted by the nominal model

$$P_m(s) = \frac{\omega_m}{I_c}(s) = \frac{K_T}{J_n s + b} \tag{7}$$

Their output difference generates a tracking error signal to tune the control parameters in the following control law:

$$u_c = \alpha \cdot I_c - \rho \cdot \omega \tag{8}$$

where α and ρ are adjusted on the basis of the Lyapunov stability theory of model reference adaptive control in the following algorithms

$$\frac{d\alpha}{dt} = k(\omega - \omega_m)\omega \tag{9}$$

$$\frac{d\rho}{dt} = -k(\omega - \omega_m)I_c \tag{10}$$

where k is the adaptation gain to be determined by the designer.

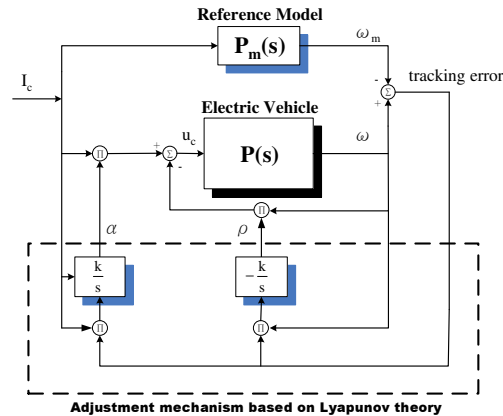


Fig. 5. Block diagram of the inner loop (MRAC) for each driving wheel.

A detailed derivation of the above equations of model reference adaptive controller based on the Lyapunov theory can be found in many text books, such as Åström [18]. The overall block diagram of the proposed EDS is presented in Fig. 6.

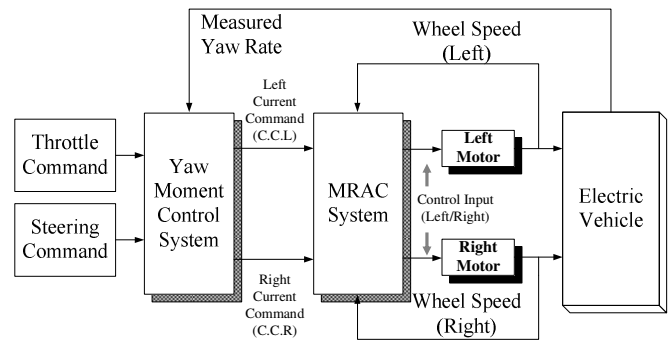


Fig. 6. Block diagram of the proposed EDS.

III. HARDWARE IMPLEMENTATION

A. Experimental Setup

To verify the effectiveness of the proposed control system, an experiment set was built on a commercial vehicle “Nissan March”, reconstructed by the Department of Vehicle Engineering at Mingchi University of Technology, which was directly driven by two rear wheel motors. These pair of wheel

motors and their electronic drives were developed in the Propulsion Control Laboratory at National Taiwan University. The motor drive was composed of two IGBT invertors controlled with the noted triangle PWM technique coded in FPGA; the switching frequency of the invertors was 10 kHz. The optimal current waveform developed by Yang *et al.* [19-21] was employed for the best driving efficiency.

The configuration of the experimental setup is depicted in Fig. 7. A rotational potential meter provides the steering command, ranging from -10V through +10V to correspond 90° through -90°; a single axis gyroscope (KRG-3) detects the vehicle yaw rate; and the accelerator pedal connects a simple circuit with a variable resistor to provide the driving command from 0V through 5V. Furthermore, the wheel speed is estimated by encoder pulse each 60 electrical degrees. The vehicle specifications and control parameters used in the following experiments are illustrated in Table I.

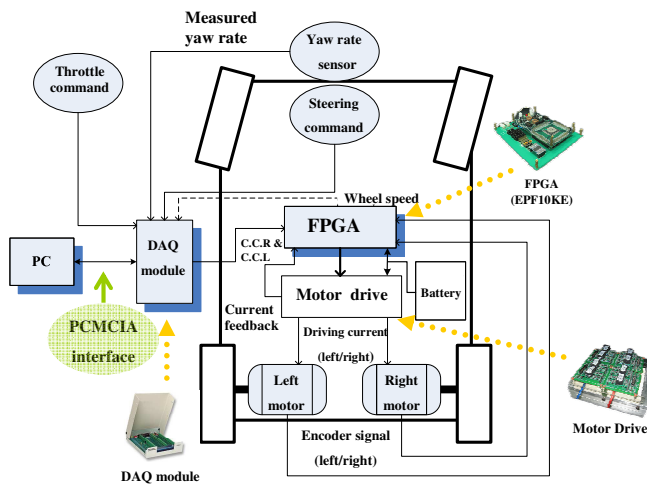


Fig. 7. Configuration of experimental setup.

TABLE I
Vehicle Specifications and Control Parameters

Vehicle specifications	
Curb mass	680 kg
Passenger	65 kg
Cornering stiffness (front) C_f	51918 N/rad
Cornering stiffness (rear) C_r	37407 N/rad
Vehicle length/width/height	345/135/148 cm
Wheelbase/thread/chassis height	220/135/ 14 cm
Control parameters	
Throttle command gain K_{CT}	10
K_p/K_i of PI controller	26/0.02
Adaptation gain k	5
Desired yaw rate model	$\gamma_d = \frac{0.51}{1+0.35s} \delta$
Reference model	$P_m(s) = \frac{0.75}{s+0.85}$

B. Implementation of EDS

As shown in Fig. 7, the proposed EDS was integrated with an EPF10KE FPGA device and a PC. In the outer loop, the yaw moment controller was realized in the PC, and transmitted the current command signals through PCMCIA interface and an A/D converter to the FPGA. In the inner loop, the MRAC system was coded in the control IC of FPGA with

Verilog HDL in the fixed-point arithmetic format, which provided a practical solution to digital signal processing due to its simple structure of logic circuit and fast software program operation. However, proper numerical scaling played a very important role in the synthesis of this kind of arithmetic process. In this study, the vehicle was only provided with 48V batteries for low speed tests.

IV. EXPERIMENTAL RESULTS

Figure 8 shows the results of straight-line motion experiment without control. The throttle command was fixed for both driving wheels and no steering command was given. It shows that the left wheel speed differs from the right, and the vehicle departs from a straight lane. As was mentioned above, the dynamics of both driving motors are not identical because of manufacturing and installation tolerance. The yaw rate also varies around a nonzero mean value.

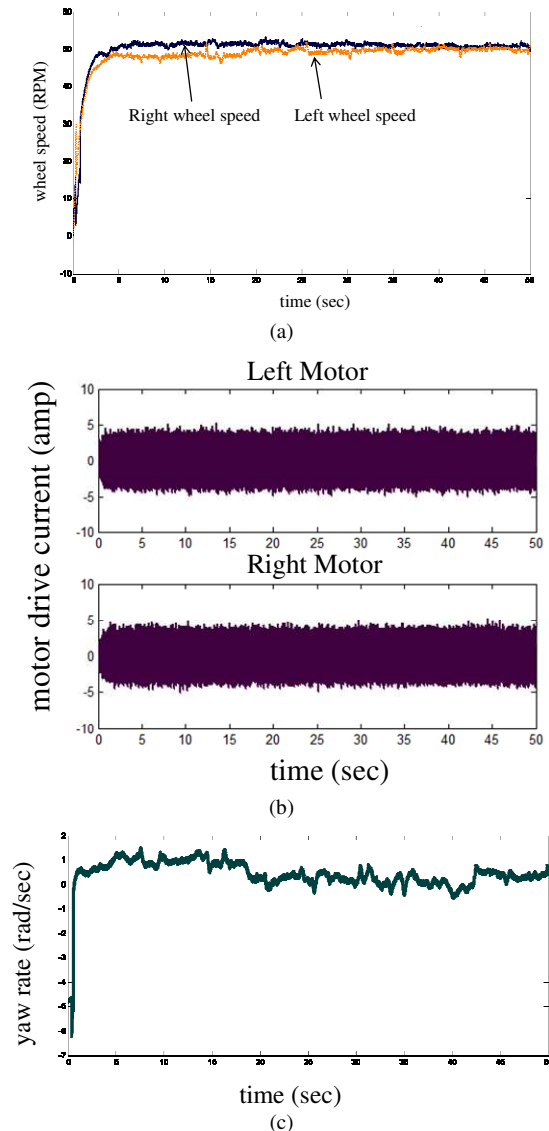


Fig. 8. Experiment Results (without control). (a) Wheel speed. (b) Motor drive current. (c) Yaw rate.

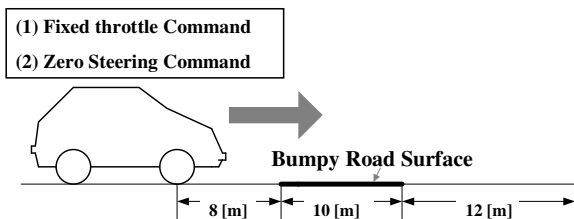


Fig. 9. Straight-line motion test on a bumpy road surface.

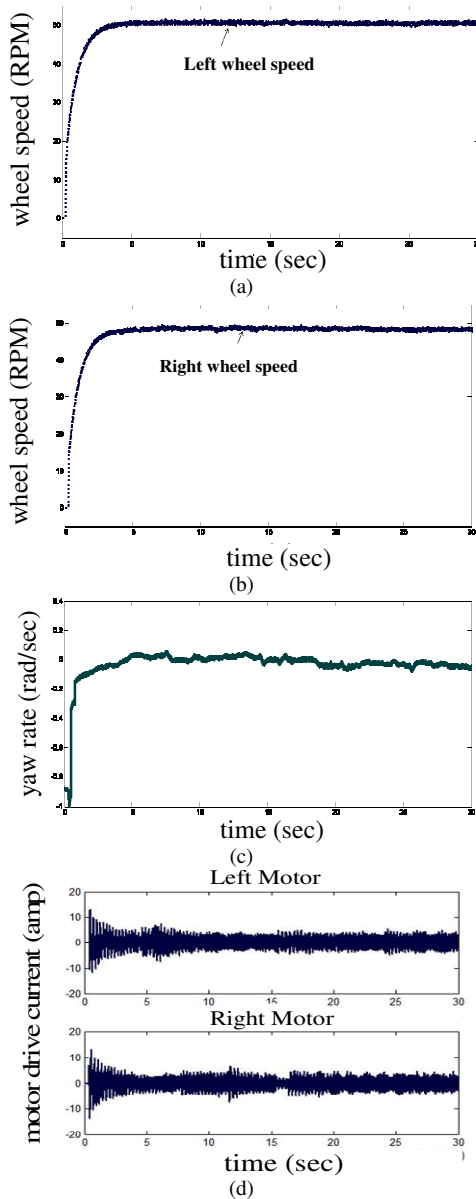


Fig. 10. Experimental Results (with control; on a bumpy road surface). (a) Left wheel speed. (b) Right wheel speed. (c) Yaw rate. (d) Driving current of motors.

With the proposed EDS, a straight-line motion experiment was investigated along a bumpy road surface covered with plastic cloth and rough canvas under one side of wheels, while keeping the road surface clean under the other side of wheels, as depicted in Fig. 9. Figure 10 shows the experimental results as the vehicle accelerated by a constant throttle command. It is observed that the EDS is able to adjust the driving currents

and keeps both driving wheels at around 49-50 rpm and the yaw rate around zero, subject to dissimilar motor dynamics and road disturbances. It demonstrates that the vehicle can successfully follow the straight path under the control.

The sequential tracking photographs represented in Fig. 11 demonstrates that the vehicle, in the long run, deviates from the straight path without control, while keeping on a straight line with the proposed electric differential control strategy.

V. CONCLUSIONS

A simple EDS has been successfully applied to an electric vehicle, with satisfactory performance. The outer control loop is able to regulate the vehicle yaw motion by tracking a desired yaw rate, and the inner loop control, designed based on the MRAC, can effectively compensate both wheel speeds of vehicle subject to motor differences and external disturbances, thereby improving system robustness. Although the yaw rate control loop requires a yaw rate sensor, the adaptive control loop distributes current to each driving wheel for eliminating the side slip angle or tracking a desired value, without using expensive side slip sensors. The experiments in this study, focusing on the straight-line motion test at a low speed, have shown satisfactory results. Further experiments for cornering and higher speed tests are in progress, and more test results are coming soon.

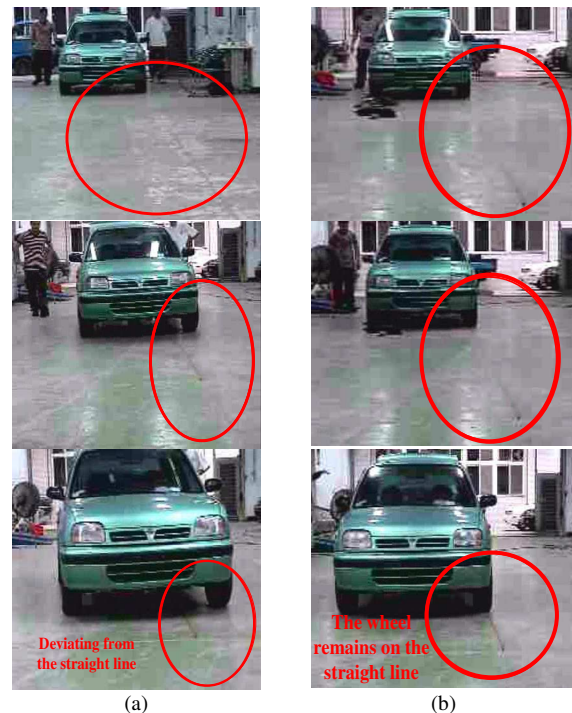


Fig. 11. Divided track of the vehicle motion. (a) without control. (b) with control (on bumpy road surface).

ACKNOWLEDGMENT

The authors would like to express their sincere thanks to D.Y. Huang and his students for their help in providing and reconstructing the test vehicle. We wish to acknowledge Prof.

B.C Chen for his valued suggestions about the vehicle dynamics and control, which is helpful for our study.

[21] Y. P. Yang and D. S. Chung, "Optimal design and control of a wheel motor for electric passenger cars," *IEEE Trans. on Magnetics*, vol. 43, pp.51-61, no. 1, 2007.

REFERENCES

- [1] M. Ehsani, Y. Gao, S. E. Gay, and A. Emadi, *Modern Electric, Hybrid Electric, and Fuel Cell Vehicles: Fundamentals, Theory, and Design*, CRC Press, 2004.
- [2] C. C. Chan, "Present status and future trends of electric vehicles," *Proc. of the IEE International Conference on Advanced in Power System Control, Operation and Management, APSCOM-93*, pp. 456-469, 1993.
- [3] C. C. Chan and K. T. Chau, *Modern Electric Vehicle Technology*, New York, Oxford Science Publications, 2001.
- [4] M. Shino and M. Nagai, "Independent wheel torque control of small-scale electric vehicle for handling and stability improvement," *JSAE Rev.*, vol. 24, pp. 449-456, 2003.
- [5] Y. Hori, Y. Toyoda, and Y. Tsuruoka, "Traction control of electric vehicle: basic experimental results using the test EV, 'UOT'," *IEEE Trans. on Industry Applications*, vol. 34, no. 5, pp. 1131-1138, 1998.
- [6] H. Sado, S. Sakai, Y. Hori, "Road condition estimation for traction control electric vehicle," *Proc. of the IEEE International Symposium on Industrial Electronics*, Bled, Slovenia, vol. 2, pp. 973-978, 1999.
- [7] S.-I. Sakai, H. Sado, and Y. Hori, "Motion control in an electric vehicle with four independently driven in-wheel motors," *IEEE/ASME Trans. on Mechatronics*, vol. 4, no. 1, pp.9-16, 1999.
- [8] K. Fujii, and H. Fujimoto, "Traction control based on slip ratio estimation without detecting vehicle speed for electric vehicle," *Power Conversion Conference*, Nagoya, Japan, pp. 688-693, 2007.
- [9] H. Fujimoto, T. Saito, A. Tsumasaka, and T. Noguchi, "Motion control and road condition estimation of electric vehicle with two in-wheel motors," *Proc. of the 2004 IEEE International Conference on Control Applications*, Taipei, Taiwan, pp. 1266-1271, 2004.
- [10] M. Shino, N. Miyamoto, Y. Q. Wang, and M. Nagai, "Dynamic driving/braking distribution in electric vehicle with independently driven four wheels," *Electric Engineering in Japan*, vol. 38, no.1, pp. 79-89, 2002.
- [11] M. Abe, K. Yoshio, S. Yasuji, F. Yoshimi, "Improvement of vehicle handling safety with vehicle side-slip control by direct yaw moment," *Vehicle System Dynamics*, vol. 33, SUPPL, pp. 665-679, 2000.
- [12] Y. Aoki, T. Uchida and Y. Hori, "Experimental demonstration of body slip angle control based on a novel linear observer for electric vehicle," *Industrial Electronics Society, IECON 2005. 32nd Annual Conference of IEEE*, Raleigh, South Carolina, pp. 2620-2625, 2005.
- [13] E. Eamailzadeh, A. Goodarzi and G. R. Vossoughi, "Optimal yaw moment control law for improved vehicle handing," *Mechatronics*, vol. 13, pp. 659-675, 2002.
- [14] A. H. Niasar, H. Moghbeli, and R. Kazemi, "Yaw moment control via emotional adaptive neuro-fuzzy controller for independent rear wheel drives of an electric vehicle," *Proceedings of 2003 IEEE Conference on Control Applications*, vol.1, p. 380-385, 2003.
- [15] T. D. Gillespie, *Fundamentals of Vehicle Dynamics*, SAE International, 1992.
- [16] M. Shino, N. Miyamoto, Y. Q. Wang, and M. Nagai, "Traction control of electric vehicle considering vehicle stability," *Proc. the 6th International Workshop on Advanced Motion Control 2000*, Nagoya, Japan, pp. 311-316, 2000.
- [17] Y. Hori, "Future vehicle driven by electricity and control-research on four-wheel-motored "UOT electric march II"," *IEEE Trans. on Industrial Electronics*, vol. 51, no. 5, pp.954-962, 2004.
- [18] K. J. Åström and B. Wittenmark, *Adaptive Control*, Addison-Wesley Publishing Company, 1995.
- [19] Y. P. Yang, Y. P. Luh, and C. M. Lee, "A novel design of optimal phase current waveform for an electric vehicle wheel motor," *Electronic Power Components and Systems*, vol. 30, pp. 705-721, 2002.
- [20] Y. P. Yang, H. P. Wang, S. W. Wu, and Y. P. Luh, "Design and control of axial-flux brushless DC wheel motors for electric vehicles-part II: optimal current waveforms and performance test," *IEEE Trans. on Magnetics*, vol. 40, pp. 1883-1891, 2004.